transitions are observed at energies below the Soret band. Gouterman and co-workers[18] assign a series of additional bands starting at 35 200 cm^{-1} to MLCT $e_g(d) \rightarrow b_{1u}(\pi^*)$ and to higher π^* levels. Using our model, with the Pc(2-)Ni(III)/Pc(2-)Ni(II) couple guesstimated to lie at 1.5 eV, we estimate the MLCT2 transition (eq 12) to lie somewhat above 29 000 cm^{-1}, depending upon the energy separation between the $e_g(d)$ level and higher filled d-orbital levels. This is in satisfactory agreement with the assignment of Gouterman.[18]

Copper(II) Phthalocyanine (Square-Planar d^9). No LMCT transitions are permissible from a_{1u} or a_{2u}. However, copper(II) does show near-infrared absorption with a sharp peak near 8300 cm^{-1}, observed initially in its crystal spectrum.[40] Interestingly, copper(II) phthalocyanine is photoconductive in this near-infrared region.[41-45]

We report the first solution spectrum of copper(II) phthalocyanine (Figure 4) showing this absorption band, which must be a trip-multiplet transition[21] since no other options are available for this ion. The similarity between this absorption spectrum band envelope and that of the near-infrared photocurrent action spectrum[45] is astonishing. Note that inelastic electron tunneling spectroscopy has been used to determine electronic transitions in a range of metallophthalocyanines and that transitions were observed at 1.23 and 1.15 eV for CoPc and CuPc, respectively, in close agreement with the absorption data reported here.[46]

Conclusions

The electrochemical model and the energy level diagram shown in Figure 2 provide a convincing interpretation of the charge-transfer spectra of first-row transition-metal phthalocyanines. The errors associated with variation in entropy from ground to excited state and the vibrational excitation of the excited state appear to be small, or to cancel, to provide remarkable agreement between observed and calculated band energies. Indeed as discussed above the apparent 0-0 nature of the LMCT bands eliminates the vibrational excitation error.

These data are important because they provide a detailed and quantitative understanding of the lower excited states of metallophthalocyanines which may ultimately find use as photocatalysts.[10] In particular, acceptance of the model allows the electronic spectra to be used as a means of calculating excited-state potentials simply by reversing the procedure outlined in this paper.[10] They are also relevant to studies in electron transfer in metalloproteins, providing parallel data to some recent studies on heme porphyrin charge-transfer spectra by Makinen and coworkers.[46]

Acknowledgment. This research is part of a joint project with Professor A. J. Bard (University of Texas at Austin) supported by the Office of Naval Research (Washington, D.C.) to whom we are indebted. Financial support from the Natural Sciences and Engineering Research Council (Ottawa) is also appreciated. We also acknowledge stimulating discussions with Professor M. Gouterman (Seattle).

(40) Schott, M. *J. Chem. Phys.* **1966**, *44*, 429-30.
(41) Harrison, S. E. *J. Chem. Phys.* **1969**, *50*, 4739-42.
(42) Day, P.; Williams, R. J. P. *J. Chem. Phys.* **1965**, *42*, 4049-50.
(43) Day, P.; Williams, R. J. P. *J. Chem. Phys.* **1965**, 236-40.
(44) Minami, N. *J. Chem. Phys.* **1980**, *72*, 6317-18.
(45) Yoshino, K.; Kaneto, K.; Tatsuno, K.; Inuishi, Y. *J. Phys. Soc. Jpn.* **1973**, *35*, 120-4.
(46) Lüth, H.; Roll, U.; Ewert, S. *Phys. Rev. B* **1978**, *18*, 4241-50.
(47) Makinen, M. W.; Churg, A. K.; Shen, Y.-Y.; Hill, S. C. Proceedings of the Symposium on the Interaction between Iron and Proteins in Oxygen and Electron Transport, Blacksburg, Va., 1980 (to be published by Elsevier).

(48) The spectrum reported in Figure 3A is the spectrum initially observed after electrochemical reduction of the chromium(III) starting material. It shows evidence of aggregation since it appears to exhibit two Q bands. After some period of time the two bands are replaced by a single Q band at an energy approximately midway between the two Q bands and with an intensity approximately twice their value. There are some concomitant changes in the cyclic voltammogram with time. We hope to provide further data on this system in due course. There is the possibility that the band near 28 000 cm^{-1}, identified as LMCT2, may possess some Soret character.

Electroreductive Alkylation of Iron in Porphyrin Complexes. Electrochemical and Spectral Characteristics of σ-Alkyliron Porphyrins

Doris Lexa,[1a] Joel Mispelter,[1b] and Jean-Michel Savéant*[1a]

Contribution from the Laboratoire d'Electrochimie de l'Université Paris 7, 75251 Paris Cedex 05, and the U-219 INSERM, Institut Curie, Centre Universitaire, 91405 Orsay, France.
Received March 30, 1981

Abstract: σ-Alkyliron porphyrins can be obtained by the reaction of electrogenerated iron(I) porphyrins on alkyl halides. The $(Fe^{II})^-R$ complex thus obtained can be oxidized electrochemically in a reversible manner into the corresponding complex $(Fe^{III})^-R$. The latter undergoes a further one-electron oxidation into a transient (formal) $(Fe^{IV})^-R$ complex. The UV-visible spectra of both the $(Fe^{III})^-R$ and $(Fe^{II})^-R$ porphyrins have been obtained. ESR and NMR spectra of the $(Fe^{III})^-R$ porphyrins show that they are low-spin complexes involving a σ-iron-carbon bond. The standard potentials of the $(Fe^{III})^-R/(Fe^{II})^-R$ couple shift negatively, parallel to those of the Fe(II)/Fe(I) couple, as the porphyrin ring becomes more electron donating. In all cases, opposite to what occurs with cobalt porphyrins, the former potential is positive to the latter, indicating a better affinity of R· toward Fe(I) than toward Fe(II). The reactivity of the iron(I) porphyrins toward RX increases with the electron-donating ability of the ring. The reaction mechanism appears more likely to be of the S_N2 type than to involve prior outer-sphere electron transfer between Fe(I) and RX.

The synthesis of metal-σ-alkyl derivatives of tetraaza-macrocyclic cobalt complexes is presently a well-documented area. These derivatives can be prepared according to three different types of reactions: carbanion transfer to Co(III) from another organometallic compound, usually Grignard or organolithium reagents;[2] addition of the alkyl radical to Co(II), the Co(II) complex generating the alkyl radical through halogen abstraction from the starting alkyl halide,[3] nucleophilic attack of the Co(I)

(1) (a) Laboratoire d'Electrochimie de l'Université de Paris 7. (b) Institut Curie, U-219 INSERM.

(2) (a) Costa, G.; Mestroni, G.; Licari, T.; Mestroni, E. *Inorg. Nucl. Chem. Lett.* **1969**, *5*, 561. (b) Costa, G. *Coord. Chem. Rev.* **1972**, *8*, 63.

0002-7863/81/1503-6806$01.25/0

Table I. Standard Potentials of the M(II)/M(I), (M^{III})-R/(M^{II})-R, and (M^{IV})-R/(M^{III})-R Couples in DMF

porphyrin complex	E° Fe(II)/Fe(I), V vs. SCE	E° (Fe^{III})-R/(Fe^{II})-R, V vs. SCE	E° (Fe^{IV})-R/(Fe^{III})-R, V vs. SCE
$Fe(C_{12}TPP)$	-1.12	CH_3, -0.84_5; C_2H_5, n-C_3H_7, n-C_4H_9, n-C_5H_{11}, n-C_6H_{13}, -0.94	n-C_4H_9, $+0.39_5$
Fe(OEP)	-1.23_5	CH_3, -0.94_5; $PhCH_2$, -0.94_5; n-C_3H_7, -1.06	n-C_4H_9, $+0.25$
Fe(DP)	-1.19	CH_3, -0.93_5; $PhCH_2$, -0.94_5	
Fe(TPP)	-1.08_5	CH_3, -0.76; $PhCH_3$, -0.76	
Co(TPP)[4f]	-0.77_5	n-C_4H_9, -1.27	

complex on alkyl halides[4] or olefins.[5] Although the same routes to the analogues of σ-alkyliron complexes could be envisaged, the question has been much less explored than in the cobalt case. For example in the important field of iron porphyrins, very few σ-alkyl or σ-aryl complexes have been reported so far. Ethyl[6a] and phenyl (or *p*-tolyl)[6] iron porphyrins have been prepared by reacting the corresponding Grignard reagents with the Fe(III) complex. Coupling of alkyl radicals with Fe(II) porphyrins has been suggested as a possible reaction path in their oxidation by alkyl halides.[7] In this connection, evidence has been provided for the transient formation of a σ-alkyliron complex derived from the reaction of polychlorinated methyl radicals on ferrodeuteroporphyrins IX in pulse radiolysis experiments.[8] On the other hand, vinyl σ complexes have been obtained by the electrochemical hydrogenation of the corresponding iron(II) carbene porphyrins, both under their Fe(III) and Fe(II) formal oxidation states.[9]

To our knowledge there has been no report so far of the formation of iron–carbon σ bonds by the direct alkylation of iron(I) porphyrins by electrophilic reagents such as alkyl halides. The one-electron reduction product of iron(II) porphyrins appears to be an iron(I) complex rather than the anion radical of an iron(II) complex on the basis of ESR spectroscopy.[10] It is therefore conceivable that it could form a σ-iron–carbon bond upon reaction with alkyl halides through either nucleophilic attack or prior generation of the alkyl radical by electron or halogen transfer followed by coupling of the alkyl radical with the ensuing Fe(II) complex. The purpose of the work reported hereafter was to investigate the formation of σ-alkyl–iron bonds in porphyrins by reaction of alkyl halides with the corresponding electrogenerated iron(I) complexes, to characterize the σ-alkyliron porphyrins thus obtained, to describe their electrochemical and spectral properties, and to give a preliminary account of the mechanism of their formation.

Results and Discussion

The experiments were carried out in DMF with Bu_4NBF_4, $LiClO_4$, or LiCl as supporting electrolytes. The working electrode was a platinum electrode for cyclic voltammetry, coulometry, preparative scale electrolysis, and spectroelectrochemistry. All potentials will be referenced to the aqueous saturated calomel electrode. The following porphyrin complexes were investigated: the usual tetraphenylporphyrin (TPP); a "basket handle" porphyrin derived from tetraphenylporphyrin and involving two 12-

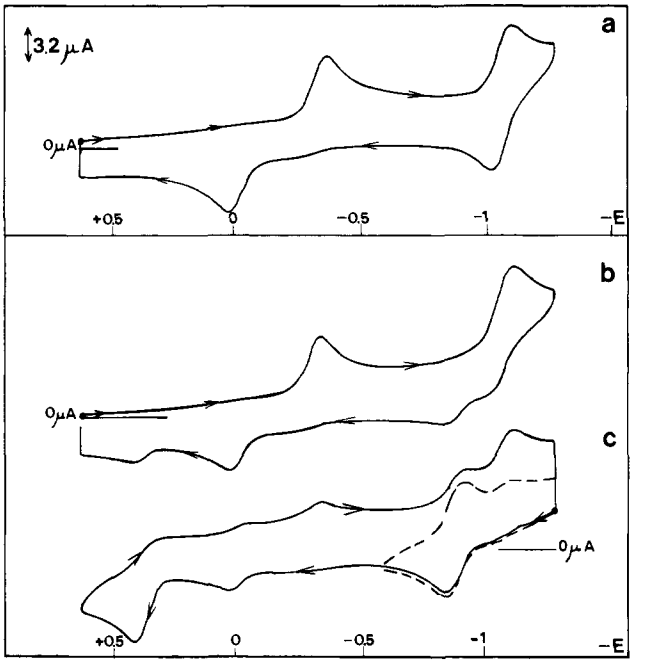

Figure 1. Cyclic voltammetry of $C_{12}TPPFeCl$ (0.9×10^{-4} M) in DMF + 0.1 M $LiClO_4$ at a platinum electrode (sweep rate = 0.2 V s^{-1}) in the absence (a) and the presence (b, c) of n-C_4H_9Br (0.83 M). Potential scanning (in V vs. SCE): (a) $+0.6 \rightarrow -1.3 \rightarrow +0.6$; (b) $+0.6 \rightarrow -1.3 \rightarrow +0.6$; (c) $-1.3 \rightarrow +0.6 \rightarrow -1.3$ (full line), $-1.3 \rightarrow -0.62 \rightarrow -1.3$ (dashed line).

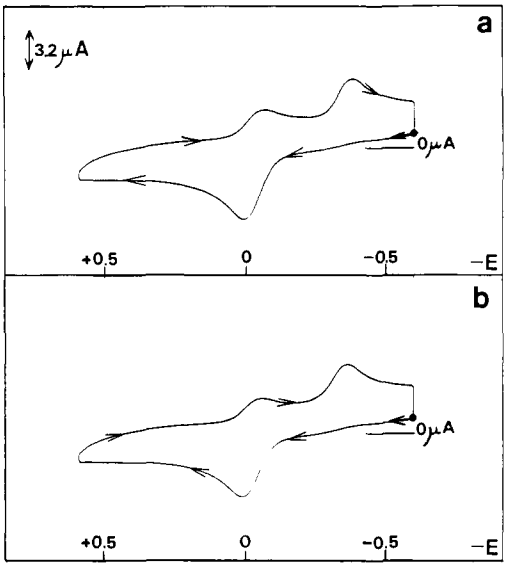

Figure 2. Cyclic voltammetry of $C_{12}TPPFeCl$ (0.9×10^{-4} M) at the first wave (from −0.6 to +0.6 V and back) in DMF + 0.1 M $LiClO_4$ at a platinum electrode (sweep rate = 0.2 V s^{-1}) in the absence (a) and in the presence (b) of n-C_4H_9Br (0.83 M).

(3) (a) Blaser, H. U.; Halpern, J. *J. Am. Chem. Soc.* **1980**, *102*, 1684 and references cited therein. (b) Goedken, V. L.; Peng, S. M.; Park, Y *J. Am. Chem. Soc.* **1974**, *96*, 284.

(4) (a) Schrauzer, G. N.; Deutsch, E. *J. Am. Chem. Soc.* **1969**, *91*, 3341. (b) Dolphin, D.; Johnson, A. W. *Chem. Commun.* **1965**, 494. (c) Pratt, J. M. "Inorganic Chemistry of Vitamin B12"; Academic Press: New York, 1972; pp 224–233 and references cited therein. (d) Momenteau, M.; Fournier, M.; Rougée, M. *J. Chim. Phys.* **1970**, *67*, 926. (e) Perret-Fauvet, M.; Gaudemer, A.; Boucly, P.; Devynck, J. *J. Organomet. Chem.* **1976**, *120*, 439. (f) Lexa, D.; Savéant, J. M.; Soufflet, J. P. *J. Electroanal. Chem.* **1979**, *100*, 159.

(5) Schrauzer, G. N.; Holland, R. J. *J. Am. Chem. Soc.* **1971**, *93*, 4060.

(6) (a) Clarke, D. A.; Dolphin, D.; Johnson, A. W.; Pinnock, H. A. *J. Chem. Soc. C* **1968**, 881. (b) Clarke, D. A.; Grigg, R.; Johnson, A. W. *Chem. Commun.* **1966**, 208. (c) Reed, C. A.; Mashiko, T.; Bentley, S. P.; Kastner, M. E.; Scheidt, W. R.; Spartalian, K.; Lang, G. *J. Am. Chem. Soc.* **1979**, *101*, 2948. (d) Ogoshi, H.; Sugimoto, H.; Yoshida, Z. "Proceedings of the 9th International Conference on Organometallic Chemistry", Dijon, France, 1979.

(7) (a) Castro, C. E. *J. Am. Chem. Soc.* **1964**, *86*, 2310. (b) Wade, R. S.; Castro, C. E. *Ibid.* **1973**, *95*, 226. (c) *Ibid.* **1973**, *95*, 231.

(8) Brault, D.; Bizet, C.; Morliere, P.; Rougée, M.; Land, C. J.; Santus, R.; Swallow, A. J. *J. Am. Chem. Soc.* **1980**, *102*, 1015.

(9) Lexa, D.; Savéant, J. M.; Battioni, J. P.; Lange, M.; Mansuy, D. *Angew. Chem., Int. Ed. Engl.* **1981**, *20*, 578.

(10) (a) Cohen, I. A.; Ostfeld, D.; Lichenstein, B. *J. Am. Chem. Soc.* **1972**, *94*, 4552. (b) Lexa, D.; Momenteau, M.; Mispelter, J. *Biochim. Biophys. Acta* **1974**, *338*, 151.

carbon aliphatic chains bound through an ether linkage to the ortho positions of two opposite phenyl rings, the cross-trans linked isomer, one chain over and the other under the porphyrin ring[11a,b] (this will be referred to as C_{12}TPP in the following); octaethylporphyrin (OEP) and deuteroporphyrin IX dimethyl ester (DP). A series of monoalkyl halides was investigated involving normal aliphatic chains and the benzyl group. All four porphyrin complexes showed qualitatively the same behavior. The main variations between them regard the exact potential location of the various redox couples and the reactivity of Fe(I) toward alkylation.

Cyclic Voltammetry. Figures 1 and 2 show the results of typical cyclic voltammetric experiments involving $FeC_{12}TPP$ chloride and *n*-butyl bromide. In the absence of the alkylating reagent, the voltammogram exhibits two successive waves featuring the Fe(III)/Fe(II) and Fe(II)/Fe(I) couples, respectively. The Fe(II)/Fe(I) wave is chemically and electrochemically reversible: the cathodic to anodic peak separation is close to 60 mV. The same is observed for the three other porphyrins, the E°'s (Table I) lying in the order TPP > C_{12}TPP > DP > OEP.[12a] The Fe(III)/Fe(II) wave has quasi-reversible character related to the difference in the thermodynamics and kinetics of the binding of counterions, here Cl^-, to the metal in the two oxidation states, Fe(III) being more readily complexed by Cl^- than Fe(II). This is more clearly seen in Figure 2a which shows the reversibility characteristics of the Fe(III)/Fe(II) wave alone. These characteristics change upon addition of chloride or other halide ions, and the overall behavior is not exactly the same when passed from one porphyrin to the other. The results of a detailed investigation of this problem will be reported elsewhere.

Upon addition of the alkyl halide, the following changes are observed. The Fe(II)/Fe(I) cathodic wave increases together with the amount of alkyl halide added up to two electrons and accordingly looses reversibility (Figure 1b,c). Simultaneously, a new reversible couple appears in front of the Fe(II)/Fe(I) wave. This is compatible to the formation of an alkyl complex by the reaction of the alkyl halide with the Fe(I) complex generated at the Fe(II)/Fe(I) wave

$$Fe(III) + 1e^- \rightleftarrows Fe(II) \quad (1)$$

$$Fe(II) + 1e^- \rightleftarrows Fe(I) \quad (2)$$

$$Fe(I) + RX \xrightarrow{k} (Fe^{III})^-R + X^- \quad (3)$$

$$(Fe^{III})^-R + 1e^- \rightleftarrows (Fe^{II})^-R \quad (4)$$

$$(Fe^{III})^-R + Fe(I) \xrightarrow{k_D} (Fe^{II})^-R + Fe(II) \quad (5)$$

which implies that, at the Fe(II)/Fe(I) wave, the alkyl complex is obtained from the $(Fe^{II})^-R$ oxidation state, corresponding to the observation that the Fe(II)/Fe(I) wave becomes a two-electron irreversible wave and the $(Fe^{III})^-R/(Fe^{II})$ R reversible couple has its standard potential less negative than that of the Fe(II)/Fe(I) couple. In other words, an ECE-type reaction scheme is functioning at the Fe(II)/Fe(I) wave in the presence of an alkyl halide. As shown earlier,[13] as soon as the newly formed chemical species, $(Fe^{III})^-R$ in the present case, is easier to reduce than the starting compound, Fe(II) in the present case, reduction of $(Fe^{III})^-R$ may occur at the electrode surface according to an ECE reaction scheme but also in the solution according to a disproportionation mechanism, the electron being then transferred from the Fe(I) complex. This problem will be further discussed in the following together with the presentation of a procedure for deriving the rate constant of the alkylation reaction (3) from cyclic voltammetric data such as those shown in Figure 1.

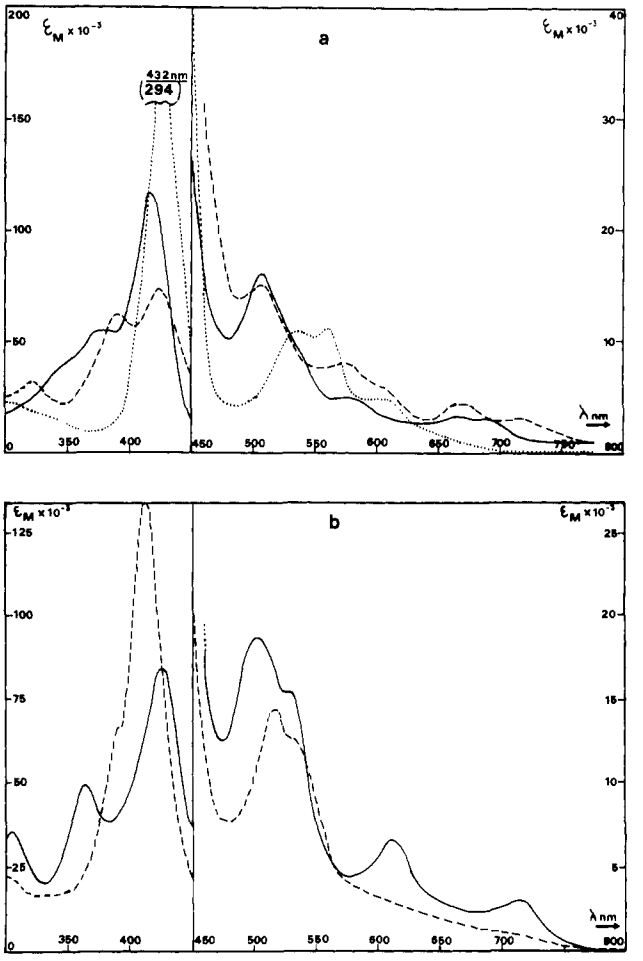

Figure 3. UV–visible spectra of nonalkylated (a) (—, $ClFe^{III}C_{12}TPP$; ···, $Fe^{II}C_{12}TPP$; - - -, $Fe^{I}C_{12}TPP$) and alkylated (b) $C_{12}TPPFe$ complexes in DMF + 0.1 M $LiClO_4$ + *n*-BuBr: (—) $(Fe^{II})^-R$; (- - -) $(Fe^{III})^-R$.

It is noted that the presumed alkyl complex formed by reaction of RX with Fe(I) has another oxidation wave in the positive potential range (Figure 1b,c). This is irreversible at low sweep rates, but reversibility appears when the sweep rate is raised and is completed at about 50 $V \cdot s^{-1}$. This wave features the transient formation of an alkyl complex having the Fe(IV) formal oxidation state. Its lifetime is on the order of 1 ms, and the Fe(IV)/Fe(III) standard potential is shown in Table I.

That Fe(II) does not react appreciably with *n*-BuBr in contrast to what occurs with Fe(I) is shown in Figure 2b, which represents an experiment in which the electrode potential was held in a region where Fe(II) is formed before being scanned anodically and then cathodically. The Fe(III)/Fe(II) wave in the presence of an alkylating agent is seen to remain the same as in the absence of an alkylating agent, showing that Fe(II) is unreactive toward RX in time ranges of at least 1 min, up to *n*-BuBr concentrations of at least 0.5 M. In the case of *n*-butyl iodide there is no appreciable reaction within the same time range up to concentrations of at least 0.10 M.

The three other porphyrins showed the same type of behavior in the presence of RX. The standard potential of the $(Fe^{III})^-R/(Fe^{II})^-R$ couple, however, varies from one porphyrin to the other (Table I), and also the reactivity of Fe(I) varies toward RX as discussed later on together with the variations of the reactivity of Fe(I) for a given porphyrin when changing the alkyl halide.

UV–Visible Spectroelectrochemistry. Figure 3 shows the UV–visible spectra obtained upon electrolysis on a platinum grid electrode in a thin-layer cell with $ClFe^{III}C_{12}TPP$ and *n*-BuBr. In Figure 3a are represented the spectra of the starting iron porphyrin under its Fe(III), Fe(II), and Fe(I) oxidation states in the absence

(11) (a) Momenteau, M.; Loock, B.; Mispelter, J.; Bisagni, E. *Nouv. J. Chim.* **1979**, *3*, 77. (b) Momenteau, M.; Loock, B. *J. Mol. Catal.* **1980**, *7*, 315.

(12) (a) This is a reflection of the increasing electron donor ability of the porphyrin ring in the series. (b) The stability of the $(Fe^{III})^-R$ complexes could probably be increased by better protection of the reaction vessels from light.[6a,b] Note also that these complexes appear to be more stable in nonpolar than in polar solvents.[6a,b]

(13) (a) Mastragostino, M.; Nadjo, L.; Savéant, J. M. *Electrochim. Acta* **1968**, *13*, 721. (b) Nadjo, L.; Savéant, J. M. *J. Electroanal. Chem.* **1973**, *48*, 113. (c) Amatore, C.; Saveant, J. M. *Ibid.* **1977**, *85*, 27. (d) *Ibid.* **1978**, *86*, 227.

Table II. Proton NMR Data for the (Fe^{III})-R Porphyrin Complexes[a]

	pyrrole H	γ-CH_2	or δ-CH_3	ε-CH_3
$C_{12}TPP$				
CH_3	−18.0, −18.4			
CH_2CH_3	−17.4, −17.5			
$CH_2CH_2CH_2CH_3$	−15.9, −18.9	+18.3	+9.7	
TPP				
CH_3	−19.1			
CH_2CH_3	−17.9			
$CH_2CH_2CH_2CH_3$	−17.7	+17.8	+10.6	
OEP				
CH_3	−1.6,[b] −2.3[c]			
$CH_2CH_2CH_2CH_3$	−1.6,[b] −2.0[c]	+16.4	+9.2	
$CH_2CH_2CH_2CH_2CH_3$	−1.6,[b] −2.0[c]	+16.5	+10.2	+5

[a] Chemical shifts (in ppm, >0 toward high fields) of the hyperfine-shifted resonance peaks at 34 °C. [b] Values for CH_2. [c] Values for CH_3.

of an alkylating agent. Electrolysis at −1.2 vs. SCE in the presence of *n*-BuBr gave rise to a spectrum featuring the alkylated complex in its (Fe^{II})-R form (Figure 3b, full line). Reoxidation at −0.8 V generates a spectrum featuring the alkyl complex in its (Fe^{III})-R form (Figure 3b, dashed line). Several oxidation–reduction cycles at these potentials could be carried out without significant changes in the spectra, showing that under careful exclusion of oxygen traces, both the (Fe^{III})-R and (Fe^{II})-R forms are stable over periods of time on the order of 1 h. Within longer time ranges both the (Fe^{III})-R and (Fe^{II})-R complexes slowly decompose into the starting Fe(II) complex which is then itself reoxidized into the Fe(III) complex by trace oxygen.[12b]

The behavior observed with other alkyl halides or other porphyrins is exactly the same. For a given porphyrin, the spectra of the (Fe^{III})-R and (Fe^{II})-R are practically the same whatever the nature of R. For $C_{12}TPP(Fe^{II})^-$ benzyl the only change is a shift of the band from 710 to 757 nm.

Coulometry. Starting with the Fe(III) complex, electrolysis in a preparative scale cell at the potential of the Fe(II)/Fe(I) wave resulted in the consumption of approximately 3 F/mol and the reoxidation at the potential of (Fe^{III})-R/(Fe^{II})-R of approximately 1 F/mol. This confirms the stoichiometry of the reactions already suggested by the cyclic voltammetric experiments. In fact the first number was constantly found to be slightly—10–20%—larger than 3 F/mol indicating slow decomposition of the (Fe^{II})-R complex during electrolysis (this currently lasted about 15 min). The second number was reproducibly found to be somewhat less than 1 F/mol, which indicates most likely a partial reoxidation of the Fe^{II}-R complex into the (Fe^{III})-R complex by trace oxygen. The solution in the preparative scale cell is indeed more difficult to protect against air penetration than that in the spectroelectrochemical thin-layer cell.[12b]

ESR and NMR Spectroscopy. ESR and proton NMR spectroscopies of the alkyl complexes were investigated with the aim of substantiating the contention that we are actually dealing with complexes involving a σ-alkyl–iron bond. The NMR experiments required the transfer of the electrolyzed solution from the preparative scale electrochemical cell into the NMR tube. It was not thus possible to completely avoid air contamination of the sample which resulted in the electrogenerated (Fe^{II})-R complex being reoxidized into the (Fe^{III})-R complex. The latter slowly decomposes into the starting Fe(II) complex, this being finally oxidized into an Fe(III) complex. This last compound was obtained in the dimeric μ-oxo form with TPP, DP, and OEP and in the monomeric form with $C_{12}TPP$, the basket handle chains preventing dimerization to occur. This sequence of events was checked by UV–visible spectroscopy with the same experimental procedure of transfer as that used for the NMR experiments. The NMR spectra presented and discussed in the following thus concern the (Fe^{III})-R complexes. The (Fe^{II})-R complex, directly generated in a spectroelectrochemical cell of the same type as that used for the UV–visible experiments and placed in the cavity of the ESR spectrometer, showed no ESR signal at 77 K. The (Fe^{III})-R complex, introduced into the ESR cell with the same procedure as that used for the NMR experiments, shows a spectrum characteristic of a low-spin ($S = {}^1/_2$) ferric complex with $g = 2.69$, 2.25, and 1.84[14] (Figure 4). These experiments were carried out with the TPP–Fe–*n*-C_4H_9 complex. The spectrum disappears upon exposure of the solution to air in the same way as that observed in the NMR experiments, showing that the observed species is the same in both cases.

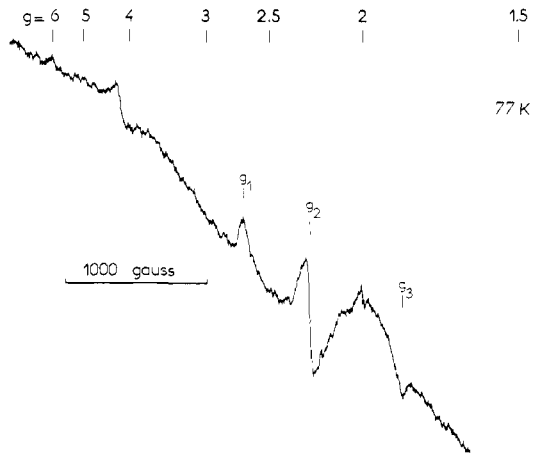

Figure 4. ESR spectrum of $TPP(Fe^{III})$-*n*-C_4H_9 at 77 K. The drift of the base line is due to the contamination of liquid nitrogen by paramagnetic oxygen. The signal near $g = 4$ is due to a nonheme iron. It was present in the spectrum before the transfer of the electrolyzed solution and after exposure of the sample to air.

The paramagnetic character of these (Fe^{III})-R complexes was confirmed by proton NMR spectroscopy. Several hyperfine shifted resonance peaks were indeed observed outside of the usual diamagnetic range comprised between 0 and 10 ppm vs. Me_4Si (Table II). This is in particular the case for pyrrole protons of TPP and $C_{12}TPP$ which give resonance peaks between −15 and −19 ppm at 34 °C. Such shifts are in agreement with a low-spin ferric structure.[14b] This is further confirmed by the comparison of the shifts observed with those of related compounds, namely, monocyanohemes (−16 ppm for the pyrrole protons in $TPP(Fe^{III})$-CN, −16.7 and −18.2 ppm for $DP(Fe^{III})$-CN at 34 °C[14c]). In the case of protoporphyrin IX, such compounds have been characterized as low-spin ferric species by magnetic susceptibility measurements in solution.[14d] It was suggested that the sixth coordinating position could be occupied by a solvent molecule (Me_2SO-d_6).[14d] A similar ligand coordination may well exist in our case since we used a complexing solvent. Furthermore, the paramagnetic shifts we observed for the pyrrole protons are not in agreement with those for a high-spin (Fe^{III})-R complex. For such species, the corresponding resonance peaks are indeed found in a +70 to +80-ppm range.[14b] The displacement then mainly results from the delocalization of the unpaired electron from the metal $d_{x^2-y^2}$ orbital into the σ framework of the porphyrin skeleton. On the contrary, the paramagnetic interaction of opposite sign observed in low-spin, ferric species is mainly a reflection of unpaired electron delocalization into the π-type orbitals of the porphyrin ring. In the case of $OEP(Fe^{III})$-R, the shifts of the methylene protons would then be expected to be opposite in sign to that observed for the pyrrole protons.[14b] In fact, the small high-field shift observed (Table II) results from two contributions of opposite signs: the

(14) (a) Palmer, G. "Electron Paramagnetic Resonance of Hemoproteins" In "The Porphyrins"; Dolphin, D., Ed.; Academic Press: New York, 1979; Vol. 4, pp 313–353. (b) La Mar, G. N.; Walker, F. A. "Nuclear Magnetic Resonance of Paramagnetic Metalloporphyrin" In "The Porphyrins"; Academic Press: New York, 1979; pp 61–157. (c) Mispelter, J., unpublished results. (d) Wang, J. T.; Yeh, H. J. C.; Johnson, D. F. *J. Am. Chem. Soc.* **1978**, *100*, 2400. (e) Mispelter, J.; Momenteau, M., unpublished results. (f) Mansuy, D.; Lange, M.; Chottard, J. C.; Bartoli, J. F.; Chevrie, B.; Weiss, R. *Angew. Chem., Int. Ed. Engl.* **1978**, *17*, 781. (g) Kurland, R. J.; McGarvey, B. R. *J. Magn. Reson.* **1970**, *2*, 286.

low-field contact shift and the pseudocontact interaction which shifts the resonance peaks of the in-plane protons toward high fields. A quantitative determination of the latter interaction cannot be made in the present case. However, its sign is given by the shift observed for some of the bridge methylene protons for $C_{12}TPP$ which where observed outside of the diamagnetic range toward the low-field region (+11.5 ppm from Me_4Si). With TPP, only one resonance peak is observed for the eight pyrrole protons, indicating that the symmetry of the tetrapyrrolic ring is conserved in the $(Fe^{III})^-R$ complex. With $C_{12}TPP$ two resonance peaks are observed, indicating a loss of the D_4 symmetry due to asymmetry vs. the plane of the ring caused concomitantly by the axial complexation and the presence of the C_{12} chains. It has indeed been observed that the $C_{12}TPP$ free base and even the Zn(II) complex show a single resonance peak for the pyrrole proton whereas two resonance peaks are observed for the $C_{12}TPPFe^{III}Cl^-$ complex.[14e] This shows that the tetrapyrrolic ring keeps the same symmetry in the Fe^{III}–R and the starting Fe(III) complexes. This is further confirmed for the case of the $OEP(Fe^{III})^-R$ complex: the methyl protons of the ethyl substituents remain equivalent while a small inequivalency (0.1 ppm) appears for the methylene protons of these alkyl groups. Here again, this is explained by the asymmetry induced by axial coordination.

The proton resonances of the phenyl groups of TPP and $C_{12}TPP$ as well as most of the CH_2 of the C_{12} chains were not visible in the spectra, most being probably hidden by the resonance peaks of the alkyl halide added in large excess and by those of the undeuterated DMF which largely mask the region between 0 and 10 ppm. In the case of methyl and ethyl complexes no other resonance peaks except those regarding the ring protons as discussed above were observed. On the contrary, for the butyl derivative and the three porphyrins TPP, $C_{12}TPP$, and OEP, two additional peaks are observed around +17 and +10 ppm (Table II) having line widths on the order of 35 and 15 Hz, respectively. The surface areas of these peaks are compatible with 2 (±1) and 3 (±1) protons, respectively, and can thus be attributed to the γ-CH_2 and δ-CH_3 protons. This is confirmed by the fact that the same signals were found in the spectrum of the *n*-pentyl complexes of the $Fe^{III}OEP$. This showed an additional peak at +5 ppm which can be attributed to the final CH_3.

These observations and rationalizations can be quantitized as follows. Taking, for example, the $TPP(Fe^{III})^-n\text{-}C_4H_9$ complex, we can estimate the successive iron–proton distances roughly as 2.4, 3.0, 4.5, and 5.5 Å starting with an Fe–C distance of 1.8 Å.[15] With the assumption that the proton relaxation has essentially dipolar character based on the line width observed for the pyrrole protons (15 Hz), the line widths for the α, β, γ, and δ protons are estimated as 2000, 500, 40, and 12 Hz, respectively. This is in agreement with the fact that the α-CH_2 and β-CH_2 signals could not be observed. The line widths calculated for the γ-CH_2 and δ-CH_3 protons are in satisfactory agreement with the experimental value, 35 and 15 Hz, respectively. Furthermore, the pseudocontact contribution to the paramagnetic shift of the two latter resonance peaks can be evaluated by starting with the *g* values obtained in the ESR spectra and the proton–iron distances as estimated above.[14g] It was found that, at 34 °C, these contributions are +12, and +7 ppm for the γ-CH_2 and δ-CH_3 protons while the experimental hyperfine shift are 16.3 and 9.6 ppm (the diamagnetic shifts are 1.5 and 0.95 ppm as obtained, e.g., from the spectrum of $n\text{-}C_4H_9Br$). This is in satisfactory agreement by taking into account the relative crudeness of the theoretical treatment. On the other hand a contact contribution cannot be excluded. This should not be, however, very significant since for a low-spin ferric complex, where the d_{z^2} orbital is not occupied, the delocalization of the unpaired electrons along the alkyl chain can only occur through hyperconjugation with the iron d_{xy} or d_{yz} orbital.

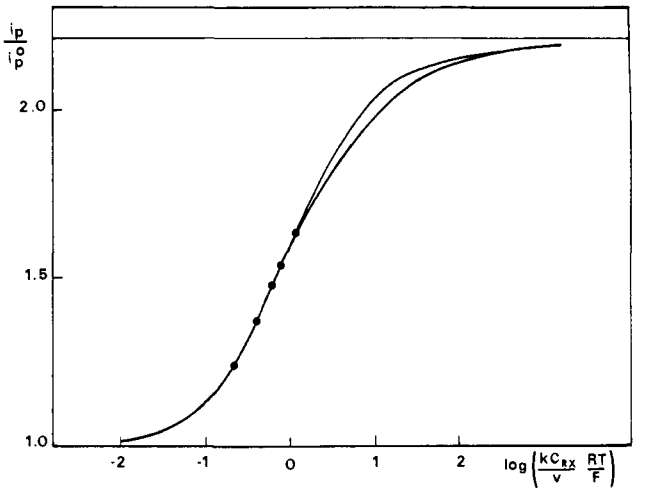

Figure 5. Kinetics of the alkylation of iron(I) porphyrins: relative increase of the Fe(II)/Fe(I) peak height as a function of the dimensionless kinetic parameter: full lines, theoretical working curves for the ECE (upper curve) and DISP (lower curve) reaction pathways; points, $C_{12}TPPFe$ in the presence of *n*-hexyl bromide; concentrations, 4.2, 7, 11, 14, and 21 × 10^{-2} M, increasing from left to right; sweep rate, 0.2 V s^{-1}.

The NMR data as interpreted in light of the ESR data thus show that the alkylated complexes do possess a σ-carbon–iron bond.

Standard Potentials of the $(Fe^{III})^-R/(Fe^{II})^-R$ and $(Fe^{IV})^-R/(Fe^{III})^-R$ Couples (Table I). For a given R group the $E°$'s become more and more negative in the series TPP > $C_{12}TPP$ > DP > OEP paralleling the order of the $E°$'s found for the Fe(II)/Fe(I) complexes. This effect similarly reflects the increasing electron-donating ability of the porphyrin ring in the series. For a given porphyrin, the $E°$'s do not depend significantly upon the nature of R with the exception of CH_3 and $PhCH_2$ which give rise to $E°$'s close to one another and about 100 mV more positive than those for the other alkyl groups. There is, in all cases, a larger stabilization of the ferric than of the ferrous state by R^- as compared to the ligand coordination of the solvent (the $E°$ for the Fe(III)/Fe(II) couple is then located around 0 V vs. SCE). The availability of the electron doublet in the methyl and benzyl carbanions being less than those for the other alkyl carbanions, this relative stabilization is less in the first case than in the second, leading to less negative $E°$'s.

A similar ring effect is found for the $(Fe^{IV})^-R/(Fe^{III})^-R$ couple. Also stabilization of the Fe(IV) state by R^- is larger than that of the Fe(III) state as compared to other ligands such as Cl^- (the Fe(IV)/Fe(III) standard potential is around 1 V for $ClFeC_{12}TPP$ in methylene chloride).

Kinetics and Mechanism of the Alkylation Reaction. The rate constants for the alkylation of the Fe(I) complexes can be derived from the increase in height of the Fe(II)/Fe(I) wave upon addition of the alkyl halide in the framework of the ECE-DISP mechanism depicted by eq 2–5.[13b,c] The relative increase in the peak current, i_p/i_p^0, as a function of the kinetic parameter $(kC_{RX}/v)(RT/F)$ is shown in Figure 5 in the form of two working curves, one for the case where the ECE completely predominates over the DISP pathway and another for the reverse situation (k is the second-order rate constant for the alkylation reaction (3), C_{RX} the concentration of the alkyl halide, and v the sweep rate). Whether one or the other situation is achieved depends upon the value of the dimensionless parameter, $p = k_D C^0 (kC_{RX})^{-3/2}(Fv/RT)^{1/2}$, where k_D is the second-order rate constant of the electron-transfer reaction (5) and C^0 the porphyrin concentration.[13c,d] In the absence of kinetic information about the electron-exchange reaction (5), it is not possible to estimate p and thus the ECE and DISP character of the overall kinetics. However, as seen in Figure 4, the two working curves are very close to one another. The use of one or the other to derive the value of k would, therefore, not lead to very different values especially if care is taken to carry

(15) This is the Fe–C distance found by X-ray spectrometry for $TPP\text{-}Fe^{II}CCl_2\cdot H_2O$.[14f] Taking a somewhat different distance, e.g., 2 Å, would not affect significantly the ensuing evaluation. The Fe–C distance was found to be 1.93 Å in a Ph–Fe complex with a somewhat different tetraazamacrocyclic ligand.[3b]

(16) Stephen, H.; Stephen, T. "Solubilities of Inorganic and Organic Compounds"; Pergamon Press: Oxford, 1963; Vol. 1, Part 2.

Table III. Rate Constants for the Reaction of the Iron(I) Porphyrins with Alkyl Halides in DMF (in M^{-1} s^{-1})

$C_{12}TPP$	n-C_4H_9Br, 25	n-$C_5H_{11}Br$, 32	n-$C_6H_{13}Br$, 40
OEP	n-C_4H_9I, 300	n-C_4H_9Br, 170	n-C_4H_9Cl 0.3
n-C_4H_9Br	OEP, 170	$C_{12}TPP$, 25	TPP, 4
CH_3Cl		$C_{12}TPP$,[a] ≃7	TPP,[a] ≃0.5
$PhCH_2Cl$	OEP, 800	DP, 260	TPP, 120

[a] Pseudo-first-order rate constants were found to be 14 and 1 s^{-1}, respectively, in experiments where gazeous CH_3Cl was bubbled through the solution under atmospheric pressure. A rough estimate of the CH_3Cl concentration is 2 M on the basis of an average value for organic solvents.[16]

out the experiments by choosing the RX concentration and the sweep rate so i_p/i_p^0 remains lower than 1.7 as was indeed done in our experiments.

Figure 5 shows how the experimental data can be fitted with the working curves and k can thus be determined as exemplified in the case of C_{12}TPPFe with n-hexyl bromide (the best fit in that case was obtained for k = 40 M^{-1} s^{-1}).

The rate constants obtained according to this procedure are listed in Table III. As expected, for a given porphyrin and a given R the order of reactivity of the halides is I > Br > Cl. In the linear aliphatic series the reactivity does not depend significantly upon the chain length with the exception of the methyl derivative which appears more reactive.

For a given halide, the reactivity of the iron(I) complex varies with the nature of the porphyrin ring parallel to the order of the Fe(II)/Fe(I) standard potentials: the more negative the E^0, the more reactive the iron(I) porphyrin. This is compatible with a mechanism involving an outer-sphere electron transfer as the first, rate-determining, step

$$Fe(I) + RX \xrightarrow{k} Fe(II) + R\cdot + X^- \qquad (3a)$$

followed by coupling either between Fe(I) and R·

$$Fe(I) + R\cdot \rightarrow (Fe^{III})^-R \qquad (3b)$$

leading directly to the reduced form of the alkyl complex or between Fe(II) and R·

$$Fe(II) + R\cdot \rightarrow (Fe^{III})^-R \qquad (3c)$$

leading to the iron(III) alkyl complex which would then be further reduced, at the electrolysis potential, through (4) or (5). In the latter case the kinetics would be of the ECE–DISP type as discussed above and of the DISP type in the first case.

This outer-sphere electron-transfer mechanism seems, however, unlikely, at least for the saturated-chain alkyl halides, according to the following reasons. Figure 6 shows log k vs. E^0 plots for electron transfer between n-C_4H_9Cl, n-C_4H_9Br, and n-C_4H_9I and a series of aromatic and heteroaromatic anion radicals in the same solvent we used in the present study.[17a] These are approximately straight lines with a slope corresponding to a transfer coefficient close to 0.5. It is seen that the rate constants observed for the reaction of $Fe^IC_{12}TPP$ with the same halides are considerably larger than those corresponding to extrapolating the straight lines down to the standard potential of the Fe(II)/Fe(I) porphyrin couple.[18]

Other mechanistic possibilities are inner-sphere mechanisms involving either halogen atom abstraction by Fe(I) followed by R·–Fe(I) coupling as in the case of the isoelectronic Co(II) complexes[3a] or S_N2 substitution of the halogen ion by the Fe(I)

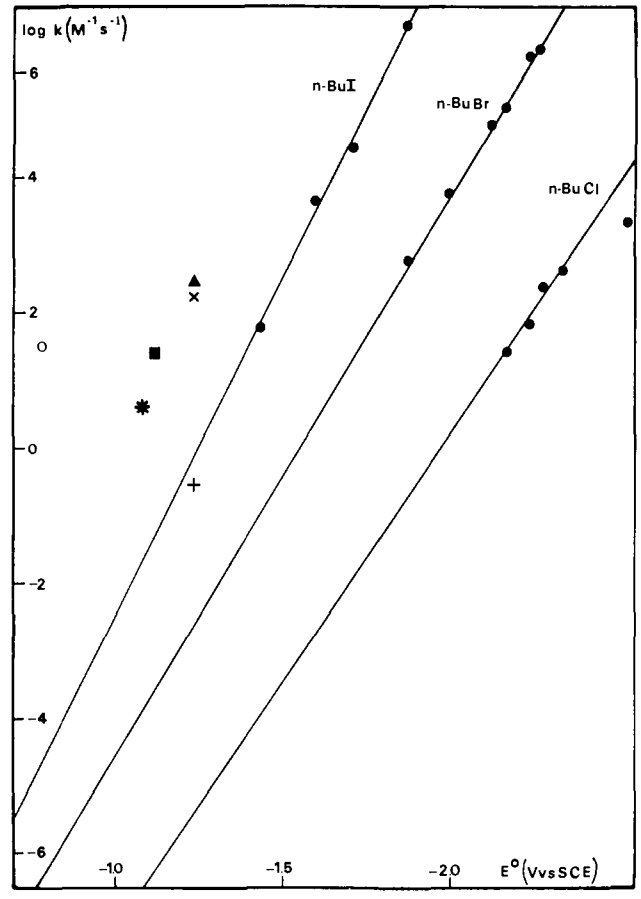

Figure 6. Reactivity of the three n-butyl halides with various nucleophiles as a function of the standard potential of the nucleophile redox couples: solid lines and points, aromatic and heteroaromatic anion radicals;[17a] n-BuBr + Fe^ITPP (*), +Co^ITPP[4f] (○), +$Fe^IC_{12}TPP$ (■), +Fe^IOEP (×), n-BuCl + Fe^IOEP (+), n-BuI + Fe^IOEP (▲).

complex. The first of these does not seem very likely in view of the unfavorable 1– charge of the iron(I) porphyrin in orienting the R–X dipole in the proper direction and of the fact that the affinity of Fe(II) toward halide ions does not appear very large as shown by the behavior of the Fe(III)/Fe(II) wave when starting from an haloiron porphyrin. This affinity of this complex is thus likely to be much less than that in the case of the isoelectronic Co(III) complexes. The S_N2 mechanism seems therefore a more plausible alternative for the present state of knowledge. This would be in agreement with the conclusions of a recent investigation of the reactivities of transition-metal nucleophiles.[19] The increased reactivity of Fe(I) when passing from TPP to $C_{12}TPP$, DP, and OEP would then be a reflection of the transmission of electron donation by the ring substituents to the central iron atom. In this context, the iron(I) porphyrins would chemically function as actual Fe(I) complexes rather than iron(II) porphyrin anion radicals in agreement with the conclusions of previous discussions based on ESR spectroscopy.[10] Note, however, that strong changes in the nature of the halide could modify the mechanism: going to easily reducible halides would favor outer-sphere electron-transfer processes. Such a trend has already been observed in the reaction of alkyl halides on the anthracene anion radical: the easier the alkyl halide is to reduce, the less the participation of the S_N2 mechanism and the more the interference of an outer-sphere electron-transfer pathway.[17] Similarly in the case of cobalt(II) tetraazamacrocyclic complexes,[3a] the halogen atom transfer mechanism appears to be replaced by an outer-sphere electron-transfer mechanism when going to easily reducible halides.

Comparison with Cobalt Complexes. There is a striking difference between iron and cobalt porphyrins in regard to the relative

(17) (a) Nadjo, L.; Savéant, J. M.; Su, K. B., to be submitted for publication. (b) Hebert, E.; Mazaleyrat, J. P.; Nadjo, L.; Savéant, J. M.; Welwart, Z. "Proceedings of the 2nd International Conference on the Mechanisms of Reactions in Solution", Cantorbery, July 1979, to be submitted for publication.

(18) Note that for an outer-sphere electron transfer, the transfer coefficient should actually vary linearly with the potential according to Marcus theory. Parabolas should thus be used instead of straight lines for the log k–E° plots. Since the curvature of these parabolas is predicted to be oriented toward the bottom of the diagram, the gap between the data for iron(I) porphyrins and the predicted rate constant would be even larger as when the potential variation of the transfer coefficient is ignored.

(19) Pearson, R. G.; Figdore, P. E. *J. Am. Chem. Soc.* **1980**, *102*, 1541.

location of the $MR/MR^{-}\cdot$ and M(II)/M(I) standard potentials: while the alkyl Fe(III) complex is easier to reduce than the Fe(II) complex, the reverse situation is observed for the case of cobalt.[4e,f] This is the reason why the electrochemical synthesis of the alkylmetal complex at the M(II)/M(I) wave leads to the $(Fe^{II})^{-}R$ complex through a $2e^{-}$ process in the first case while it gives directly the $(Co^{III})^{-}R$ complex through a $1e^{-}$ process in the second.

The difference in standard potentials between the M(III)/M(II) and $(M^{III})^{-}R/(M^{II})^{-}R$ varies considerably from iron to cobalt ($\sim$0.8 V for Fe and $\sim$1.5 V for Co[4e,f,20]), showing that the relative stabilization of the III state vs. the II state by R^{-} as compared to the ligand coordination of the solvent is much larger in the case of cobalt than in the case of iron in agreement with the softer Lewis acid character of Co(III) as compared to Fe(III).

Another approach to the same structural problem is to compare the ΔE^{0}'s between the Fe(II)/Fe(I) and $(Fe^{III})^{-}R/(Fe^{II})^{-}R$ couples, the latter being better represented as $Fe^{II}\cdot R/Fe^{I}\cdot R$ for this purpose. ΔE^{0} is $\sim$−0.2 V for Fe and $\sim$+0.5 V for Co. This points to a larger affinity of R· for Fe(I) than for Fe(II) and for Co(II) rather than for Co(I) in agreement with Fe(I) and the isoelectronic Co(II) possessing an odd number of electrons, this affinity being further modulated by the nucleophilic character of Fe(I) as compared to that of Co(II).

We also note that the reactivity of Co(I) toward a given alkyl halide appears larger than that of the corresponding Fe(I) with the same porphyrin ring: $k = 30\ M^{-1}\ s^{-1}$ for $Co^{I}TPP$ and $n\text{-}C_4H_9Br$,[4f] $k = 4\ M^{-1}\ s^{-1}$ for $Fe^{I}TPP$ with the same alkyl halide. It is expected that Co(I) be a stronger nucleophile than Fe(I). The difference in reactivity is, however, not very large. Note that the mechanism for the nucleophile displacement of the halide by the cobalt(I) porphyrins is likely to be of the S_N2 type for the same reasons as those discussed for the Fe(I) complexes (see Figure 6).

Conclusions

The main conclusions which emerge from the preceding results and discussions are the following.

(i) It is possible to form σ-alkylironporphyrins by direct alkylation of the corresponding electrogenerated iron(I) complexes. These are obtained, at the potential of Fe(I) generation, in the form of $(Fe^{II})^{-}R$ complexes. The corresponding $(Fe^{III})^{-}R$ complexes can be obtained by electrochemical oxidation of the $(Fe^{II})^{-}R$ derivatives.

(ii) ESR and proton NMR spectroscopy show that the $(Fe^{III})^{-}R$ derivatives are low-spin complexes containing a σ-iron–carbon bond.

(iii) The $(Fe^{III})^{-}R$ complexes can be electrochemically oxidized around +0.4 V vs. SCE into transient species having the formal oxidation state $(Fe^{IV})^{-}R$ and the lifetime in DMF in the range of 0.1–1 ms.

(iv) The $(Fe^{III})^{-}R/(Fe^{II})^{-}R$ couple has a standard potential positive to that of the Fe(II)/Fe(I) couple and in contrast to what occurs with the corresponding cobalt complexes. This indicates a better affinity of the R· radical for iron(I) than for iron(II) while an opposite situation is found for cobalt.

(v) The kinetics of the substitution reaction indicate that its mechanism is more likely to have S_N2 character than to be initiated by an electron-transfer reaction between the Fe(I) complex and the alkyl halide.

Experimental Section

Chemicals. DP and OEP were from commercial origin. TPP and $C_{12}TPP$ were prepared and purified according to previously described procedures.[11a,b] The alkyl halides, solvents, and supporting electrolytes were reagent grade products from commercial origin. They were used as received.

Electrodes and Cells. A three-electrode configuration was used in all cases with the reference electrode being an aqueous saturated calomel electrode and the counterelectrode a platinum wire or foil. The solutions were degassed by U grade argon. For NMR solutions the aqueous saturated calomel electrode was filled with heavy water. The solvent was DMF (DMF-d_7 for NMR) containing 0.1 M, $LiClO_4$, LiCl, or NBu_4BF_4 as the supporting electrolyte. For cyclic voltammetry the working electrode was a platinum disk of about 3.14-mm^2 surface area. For UV–visible spectroelectrochemical experiments, a thin-layer cell of 0.5 mm thickness was used with a platinum grid as the working electrode. The cell used for preparation electrolysis was a two-compartment cell with a Nafion membrane separator, the working electrode being a platinum grid foil or a mercury pool. The electrolyzed solution was then transferred under increasing argon pressure into the degassed NMR or ESR tube through Teflon pipe.

Instrumentation. For cyclic voltammetry, the instrumentation was the same as that already described.[21] A Tacussel PRT20 potentiostat was used for the preparative scale experiments with a Tacussel I65 integrator for coulometry. The proton NMR spectra were recorded at 34 °C on a Varian XL-100 spectrometer operating at 100 MHz in the Fourier transform mode. The chemical shifts were referenced to internal Me_4Si. The ESR spectra were recorded at the temperature of liquid nitrogen (77 K) on a Varian V-4502 spectrometer.

Acknowledgment. This work was supported in part by the CNRS (Equipe de Recherche Associée No. 309 "Electrochimie Moléculaire") and by the INSERM (U-219). Dr. Michel Momenteau (Institut Curie, U-219 INSERM) is gratefully thanked for the gift of $C_{12}TPP$ samples.

(20) Lexa, D. Thesis, The University of Paris, 1972, No. A07123.

(21) Lexa, D.; Savéant, J. M. *J. Am. Chem. Soc.* **1976**, *98*, 2652.